Published in final edited form as:
J Immunol. 2017 July 01; 199(1): 304–311. doi:10.4049/jimmunol.1600960.

Interleukin-6 signaling regulates small intestinal crypt homeostasis

Victoria Jeffery[†], **Andrew J. Goldson**[*], **Jack R. Dainty**[††], **Marcello Chieppa**[‡], and **Anastasia Sobolewski**[1,*,†,#]

[†]School of Biological Sciences, University of East Anglia, Norwich, Norfolk NR4 7TJ, United Kingdom

[*]Gut Health and Food Safety Institute Strategic Program, Institute of Food Research, Norwich, Norfolk, NR4 7UA, United Kingdom

[††]Norwich Medical School, University of East Anglia, Norwich, Norfolk NR4 7UQ, United Kingdom

[‡]Laboratory of Experimental Immunopathology, IRCCS De Bellis, Italy

[1]School of Pharmacy, University of East Anglia, Norwich, Norfolk NR4 7TJ, United Kingdom

Abstract

Gut homeostasis is a tightly regulated process requiring finely-tuned complex interactions between different cell types, growth factors or cytokines and their receptors. Previous work has implicated a role for interleukin (IL-6) and mucosal immune cells in intestinal regeneration following injury and in promoting inflammation and cancer. We hypothesized that IL-6 signaling could also modulate crypt homeostasis. Using mouse in vitro crypt organoid and in vivo models this study first demonstrated that exogenous IL-6 promoted crypt organoid proliferation and increased stem cell number through pSTAT3 activation in Paneth cells. Immunolabelling studies showed that the IL-6 receptor was restricted to the basal membrane of Paneth cells both in vitro and in vivo and that the crypt epithelium also expressed IL-6. Either a blocking antibody to the IL-6 receptor or a neutralising antibody to IL-6 significantly reduced in vitro basal crypt organoid proliferation and budding, and in vivo significantly reduced the number of nuclei and the number of Lgr5EGFP positive stem cells per crypt compared to IgG treated mice, with the number of Paneth cells per crypt also significantly reduced. Functional studies demonstrated that IL-6-induced in vitro crypt organoid proliferation and crypt budding was abrogated by the Wnt inhibitor IWP2. This work demonstrates that autocrine IL-6 signaling in the gut epithelium regulates crypt homeostasis through the Paneth cell and the Wnt signaling pathway.

Introduction

The intestinal epithelium is the most rapidly renewing tissue in the body with the entire epithelium being replaced every 5-7 days. This renewal takes place by way of Lgr5 positive stem cells located at the base of intestinal crypts; stem cells proliferate, migrate along the

[#]Corresponding Author: a.sobolewski@uea.ac.uk, Tel: +44(0)1603 591448.

The authors have no conflicts of interests to declare.

Europe PMC Funders Author Manuscripts

crypt-villus axis, differentiate (into Tuft cells, enteroendocrine cells, Paneth cells, enterocytes, goblet cells) and are shed into the gut lumen (1). Epithelial Paneth cells through the secretion of Wnts play a major role in the maintenance of the crypt stem cell niche (2). Previous work has also shown that other growth factors and cytokines, as well as immune cells are key in modulating epithelial stem cell-driven tissue renewal during homeostasis (3–8). Understanding the mechanisms by which these pathways are regulated in the epithelium through autocrine (and paracrine) signaling is not fully understood.

Seminal work in the *Drosophila* gut has shown regenerative responses following infection are regulated by JAK/STAT (Janus kinases / signal transducer and activator of transcription) signaling in gut epithelial stem cells through the release of enterocyte-derived Upd3, an IL-6-like cytokine (9, 10). In the mammalian gut both interleukin-6 and STAT3 have been shown to play a role in proliferation of the colonic epithelium following injury and to promote the survival of epithelial cells (11–14) during inflammation and inflammatory bowel disease (15, 16).

IL-6 is a pleiotropic cytokine involved in a plethora of cellular and immune responses in health, disease and cancer (17–19). IL-6 signaling involves the convergence of a number of signaling components (20). IL-6 first binds to a membrane bound non-signaling α-receptor IL-6 (mbIL-6R) located on the target cell. Next this IL-6R/IL-6 complex binds to the ubiquitously expressed type I transmembrane transducer protein gp130 which results in activation of downstream signaling components JAK / STAT, ERK and PI3K signaling pathways. Cells that express both the IL-6R and gp130 are responsive to IL-6; this is termed *classic signaling* and is traditionally associated with homeostasis. IL-6 can also signal *via trans-signaling*, where soluble IL-6 receptor (sIL-6R), shed from the cell membrane *via* proteolytic cleavage of a membrane-bound precursor, binds to IL-6. This IL-6 / sIL-6R complex can then activate IL-6 signaling in any cell expressing gp130; this trans-signaling pathway is associated with inflammation and cancer (21).

The aim of this study was to determine whether IL-6 *classic signaling* could modulate small intestinal crypt homeostasis. This work demonstrates a previously unidentified role for autocrine IL-6 signaling in the maintenance of the crypt stem cell niche, though the differential expression of the IL-6 receptor and downstream STAT3 signaling in Paneth cells and the Wnt signaling pathway.

Experimental Procedures

Mice and *in vivo* studies

LGR5-EGFP-Ires-CreERT2 (Jackson Labs) or C57BL/6, aged 8-12 weeks were used. Generation and genotyping of the LGR5-EGFP-Ires-CreERT2 allele has been described previously (1). All animal experiments were conducted in accordance with the Home Office Animals Scientific procedures Act of 1986 with approval of the University of East Anglia Ethical review Committee, Norwich, United Kingdom and under Home Office project licence number 80/2545. Blocking antibodies for IL-6 and IL-6 receptor or IgG controls (BioXcell) were administered to mice 3 times on alternate days by intraperitoneal injection at a concentration of 58 μg/g. Animals were euthanized by Schedule One approved methods

on day 6, and tissue processed immediately. In addition, small intestinal tissue from IL-6 knockout mice (Jackson Labs B6.129S2-Il6tm1Kopf/J), was used to count the number lysozyme positive cells per small intestinal crypt.

Reagents

Crypt culture media and supplements; Advanced DMEM/F12, Glutamax and B27 and N2 were purchased from InVitrogen. Murine recombinant epidermal growth factor, noggin and IL-6, IL-22 were all obtained from Peprotech and mouse recombinant R-spondin 1 from R & D Systems. Growth factor-reduced Matrigel was purchased from VWR International.

Immunolabelling; primary and secondary antibodies; rat anti-BrdU (Abcam), mouse anti-Lysozyme (Abcam); goat anti-E-cadherin (R&D); rabbit IgG, rabbit anti IL6 receptor and anti-IL-6 (Bio-Xcell), rabbit anti-pSTAT3 Tyr705, pSTAT3 Y705 blocking peptide, rabbit anti-Cleaved caspase-3 (Cell Signaling); Immunolabelling was visualised by using an appropriate combination of species-specific Alexafluor-conjugated secondary antibodies (488, 568, and 647 nm), raised in mouse, donkey or goat (Invitrogen). FITC-conjugated *Ulex europaeus* Lectin (UEA-1 FITC) was purchased from Sigma. Vectashield mounting medium with DAPI was purchased from Vector Laboratories Ltd. STATTIC and IWP2 were purchased from Tocris Bioscience.

Crypt isolation and culture

Small intestinal crypts were isolated from the proximal small intestine of LGR5EGFP mice as previously described (2). Briefly, the mouse small intestine was opened longitudinally, washed with phosphate buffered saline (PBS), cut into 2-4 mm pieces and incubated with 1mM EDTA in PBS (pH7.4) for 30 mins at 4°C. Crypts were liberated by serial rounds of pipetting in ice cold PBS and removal of the crypt enriched supernatant; the solution was then filtered through a 70μm cell strainer followed by centrifugation. Fifty to one hundred crypts were embedded in a 200μl droplet of growth factor reduced-Matrigel (VWR) and seeded on No. 0 coverslips (VWR) contained within a 12 well plate (Nunc). After polymerisation at 37°C for 5-10 mins, crypts were flooded with 0.5 ml of mouse crypt culture medium (MCM): advanced F12/DMEM containing B27, N2, n-acetylcysteine (1 mM), HEPES (10 mM), penicillin/ streptomycin (100 U/ml), Glutamax (2mM), epidermal growth factor (50ng/ml), noggin (100 ng/ml) and R-spondin 1 (1 μg/ml).

In IL-6 neutralising or IL-6 receptor blocking antibody experiments crypts were incubated for the entire 48 hour period in MCM and appropriate antibody or respective IgG control before addition of BrdU (1μM) for 17 hours.

Following 48 hours culture with MCM crypts were stimulated with IL-6 at concentrations of 10 ng / ml to 1μg / ml for 15mins to 17 hours for pSTAT3 experiments and for proliferation experiments placed into 10% MCM for 5 hours and after which BrdU (1μM) was added for 17 hours. For STAT3 inhibition studies, crypts were pre-incubated with STATTIC (20μM) or IWP2 (5μM) for 1 hour prior to addition of IL-6 (100ng / ml) stimulation for 17 hours (as described previously).

For pSTAT3 activation studies, the IL-6 neutralising antibody was pre-incubated with IL-6 (100ng / ml) for 1 hour before addition to the crypts for 1 hour. For receptor antibody studies, crypts were pre-incubated for 1h with the IL-6 receptor blocking antibody before addition of IL-6 (100ng / ml) for 1 hour. The same protocol was used for proliferation experiments, prior to the addition of IL-6 and BrdU (1μM) 17 hours.

For chronic IL-6 stimulation, crypts were incubated for 5 days with MCM containing 100ng / ml IL-6 before addition of BrdU (1μM) for 17 hours; media was changed every 2 days.

Immunolabelling

Mouse Lgr5EGFP small intestines were fixed in 4% paraformaldehyde, frozen in isopentane and stored at -20°C. Following the culture period small intestinal crypts were fixed with 4% paraformaldehyde. Eight to 20 μm cryosections of small intestinal tissue (Leica CM 1100C cryostat) or small intestinal crypts were permeabilized with 0.5% Triton–X (Sigma), blocked with 10% FBS, and stained with primary antibodies diluted (1:100) in PBS overnight at 4°C followed by the corresponding secondary fluorescence-conjugated antibodies (1:200 in PBS) for 2 hours as previously described (3, 4, 22).

Microscopy

Following immunofluorescent staining, samples were visualised by laser scanning confocal (Zeiss 510 META) or epifluorescence (Nikon Ti) microscopy. For confocal microscopy a X40 1.3 NA oil objective or X63 1.4NA 0.75 mm WD oil immersion objective was used to obtain confocal images. Image stacks were taken at 1-3 μm intervals, which allowed selection of precise focal planes). A X40 1.1 NA oil objective was used to image samples on the epifluorescent microscope.

Image analysis

For all experiments, between 20 and 100 crypts (*in vivo*) / organoids (*in vitro*) were counted per condition and each experiment was performed at least three separate times.

In vitro: Image-J software was used to count the total number of DAPI labelled cell nuclei in the crypt equatorial plane and the number of cells that were positive for BrdU or Lgr5EGFP was then expressed as a percentage of the total nuclei number. For semi-quantitative analysis of pSTAT3 activation, regions of interest were drawn around the entire Paneth cell nuclei and the average fluorescence intensity of the region calculated.

In vivo: Lgr5EGFP stem cells, lysozyme or UEA-1 positive Paneth cells were counted by taking a z-stack across the equatorial plane of the crypt and counting the number of nuclei in this stack that were positive for each marker. To determine the crypt length and villus height *in vivo*, at least 25 well orientated crypts and villi were measured using the segmented line tool (Fiji 1.50e) from three animals in each treatment group.

mRNA isolation and quantification

Isolation; RNA from freshly liberated or cultured small intestinal crypts, was isolated using the Isolate II RNA mini kit (Bioline). Total RNA yield was determined using a NanoDrop ND-1000 spectrophotometer (Thermo Fischer Scientific) and purity assessed by the ratio of absorbance at 260 and 280 nm. cDNA was generated from 0.5 μg RNA using the RT^2 First Strand cDNA synthesis kit (Qiagen).

Quantification; End-point PCR reactions were performed in a final volume of 25 μl, comprising 200 nm forward and reverse primers, 200 μM dNTP, 0.5 U Taq polymerase, PCR buffer (Roche), 2.5 mM $MgCl_2$, 0.5 μl cDNA using a Tprofessional TRIO thermal cycler (Biometra) with the following thermal profile: one cycle at 94°C for 3 mins, 30 cycles at 94°C for 25 s, 58°C for 30 s, and 72°C for 50 s and 1 cycle at 72°C for 5 mins. The Primer sequences used are listed were as follows; IL-6 Forward primer: GCTACCAAACTGGATATAATCAGGA; Reverse primer: CCAGGTAGCTATGGTACTCCAGAA. PCR products were run on a 2% agarose gel visualised by ethidium bromide staining.

Statistics

Experiments were performed at least three times. Data are expressed as mean ± standard error and significance determined by a student's t-test or by one-way analysis of variance with post-hoc Tukey analysis, with P values less than 0.05 considered significant.

Results

IL-6 stimulates proliferation of small intestinal organoids *via* a STAT3-mediated signaling pathway

First we determined the effect of exogenous IL-6 on the BrdU incorporation of small intestinal organoids through immunofluorescence microscopy (Figure 1A). IL-6 caused a significant increase in incorporation of BrdU at 10 and 100 ng / ml IL-6 but exhibited a dome-shaped response curve at higher concentrations (1000 ng / ml) (Figure 1B). Using the specific STAT3 inhibitor STATTIC we demonstrated that the increased BrdU incorporation induced by IL-6 was significantly reduced compared to IL-6 alone (Figure 1C). There was no effect of STATTIC on basal proliferation, which was in contrast with the effects of chronic treatment with STATTIC, where a significant decrease in BrdU incorporation compared to control was observed (Supplemental Figure 1A). Organoid survival following STATTIC treatment in the presence or absence of IL-6 was comparable to control (DMSO Control 74.9 ± 3.9; STATTIC 73.7 ± 4.5; IL-6 63.1 ± 4.9; STATTIC + IL-6 69.5 ± 4.7). However, there was a small but significant (n=3, $^{**}p<0.01$) effect of STATTIC on the percentage of caspase 3 positive cells per crypt compared to control (DMSO Control 3.6 ± 0.4; **STATTIC 6.0 ± 0.7; IL-6 2.2 ± 0.4; STATTIC + IL-6 4.8 ± 0.7). A significant increase in BrdU incorporation was observed following chronic IL-6 stimulation (Supplemental Figure 1B).

IL-6 induces activation of nuclear pSTAT3 in Paneth cells of the small intestine *via* differential expression of the IL-6 receptor

We next investigated the effect of IL-6 on pSTAT3 activation in the small intestinal epithelium using immunolabelling and visualisation of pSTAT3 activation by confocal microscopy. Following 1 hour stimulation with IL-6 (100 ng /ml), we observed pSTAT3 (green) in the nucleus (red) of UEA-1 (pink) and lysozyme (blue) positive cells, which was abrogated by a blocking peptide to pSTAT3 (Figure 2A). No fluorescent labelling was observed in IgG controls for the lysozyme antibody (Supplemental Figure 1C). Following IL-6 stimulation all UEA-1 lysozyme positive cells in a crypt domain were positive for nuclear pSTAT3 (See projection Figure 2A). All lysozyme positive cells were UEA-1 positive and characteristic of Paneth cells (23). Whilst the majority of control organoids expressed no pSTAT3 (Figure 2B), nuclear pSTAT3 activation in UEA-1 positive cells was observed in 9 out of 113 control organoids counted. Time course studies showed that maximal activation of nuclear (red) pSTAT3 (green) in UEA-1 positive (pink) Paneth cells occurred at 30 mins, and persisted at 1 and 3 hours post-stimulation (Figure 2B). Semi-quantitative analysis showed the level of nuclear pSTAT3 activation remained significantly higher than control levels 1 and 3 hours after IL-6 stimulation. Results also showed that pSTAT3 phosphorylation levels at 1 hour were the same for 100ng /ml or 1000 ng / ml IL-6 (Figure 2C).

The localization of the IL-6 receptor (red) in organoids was restricted to the basal membrane of lysozyme positive (green) cells of the small intestine *in vitro* (Figure 2D), no fluorescence was observed in the IgG control for lysozyme (Supplemental Figure 2D). Furthermore, *in vivo* labelling of the IL-6 receptor displayed the same distribution as in the *in vitro* crypt organoid cultures (Figure 2E) with basal epithelial IL-6 receptor expression constrained to the lysozyme positive cells (green) and on the membrane of their intracellular granules (Figure 2F). No IL-6R was expressed on Lgr5EGFP positive stem cells (cyan). The small intestinal crypt *in vitro* model was therefore considered a relevant *in vitro* model to study IL-6 signaling in the small intestinal crypt epithelium.

Next, we demonstrated the ability to modulate the IL-6 STAT3 signaling axis in small intestinal organoids utilizing a receptor blocking antibody to IL-6 or neutralising antibody to IL-6. Either of these antibodies in combination with IL-6 abrogated the IL-6 induced phosphorylation of STAT3 (Supplemental Figure 1J-M).)

Autocrine IL-6 signaling in the small intestinal epithelium modulates crypt cell proliferation *in vitro*

The next step was to determine whether autocrine IL-6 signaling played a role in crypt homeostasis. We first used conventional PCR to demonstrate the expression of IL-6 mRNA in crypts *in vivo* using freshly isolated (0 h) and in *in vitro* cultured (48 h) small intestinal crypts (Figure 3A). Immunofluorescent studies showed that IL-6 protein (red) was localised inside epithelial cells towards the basal pole as well as extracellularly in discrete pools around the crypt basal membrane, see white arrows (Figure 3B). We next utilised a blocking antibody to the IL-6 receptor or a neutralising antibody to the IL-6 cytokine in crypt organoid cultures and assessed basal BrdU incorporation (Figure 3C and D respectively) and

observed a significant decrease in the percentage of crypt nuclei incorporating BrdU compared to the respective IgG controls with both antibodies.

We also confirmed that the antibodies could functionally block IL-6 signaling in organoids. Incubation of either an IL-6 receptor blocking or an IL-6 neutralising antibody with IL-6 significantly decreased BrdU incorporation of organoids compared to IL-6 stimulation alone (See Supplemental Figure 1 D and E). Caspase 3 (used as a measure of cell death), and organoid survival was unaffected by either of these antibody treatments compared to IgG control organoids (Supplemental Figure 1 F-I).

Lack of gut phenotype in IL6KO mice

In order to understand the effects of perturbation of the IL-6 signaling pathway *in vivo*, tissue was obtained from IL-6 knockout mice. No difference was observed in the number of lysozyme positive cells per crypt, crypt length and the number of nuclei per crypt in IL6KO tissue compared to WT tissue (Supplemental Figure 2A-C). Furthermore, using immunolabelling, low levels of pSTAT3 were detected in some UEA-1 positive cells at the base of the crypts in both WT and IL-6 KO small intestine (Supplemental Figure 2J and K). We confirmed the specificity of the pSTAT3 antibody labelling by using a blocking peptide to pSTAT3, which abrogated the pSTAT3 signal in the UEA-1 positive cells (See Supplemental Figure 2I).

IL-6 signaling axis modulates Lgr5EGFP stem cell number *in vitro* and *in vivo*

As intestinal stem cells drive the renewal of the crypt epithelium we examined the effects of modifying the IL-6 signaling-axis on crypt stem cells both *in vitro* and *in vivo*. In addition to the observed increase in the small intestinal organoid proliferation *in vitro*, we also demonstrated that the percentage of Lgr5EGFP positive nuclei per organoid (Figure 4A) was significantly increased compared to control. Furthermore, the average number of new buds per small intestinal organoid, also a measure of stem cell number, was also significantly increased compared to control, an effect that was abrogated by STAT3 inhibition with STATTIC (Figure 4B). The use of an IL-6R blocking antibody also caused a significant reduction in the budding of small intestinal crypts (Figure 4C). Complementary *in vivo* studies using Lgr5EGFP mice treated with the IL-6 receptor blocking antibody caused a significant reduction in the number of Lgr5EGFP cells per crypt**,** the number of crypt nuclei, crypt length and villus height compared to IgG treated mice (Figure 4D-G respectively). Similar findings were obtained after mice were treated with an IL-6 neutralising antibody with a significant reduction in the number of Lgr5EGFP cells per crypt, the number of crypt nuclei and villus height compared to IgG treated mice (Figure 4H, I, K). No significant difference was observed in crypt length between mice treated with a IL-6 neutralising antibody or control IgG. (Figure 4J). Furthermore, both the IL-6 receptor blocking antibody and the neutralising IL-6 antibody caused a significant reduction in the number of lysozyme (Figure 4L and N) and UEA-1 (Figure 4M and O) positive cells per crypt compared to the respective IgG treated mice. Representative confocal images from mouse *in vivo* antibody experiments including Lgr5EGFP, lysozyme, UEA-1, Ki67 and caspase 3 labelling are included in Supplemental Figure 2E-H.

IL-6 induces crypt cell proliferation through a Wnt signaling pathway

Paneth cells have been shown to be a major source of Wnts and the Wnt signaling pathway is a master regulator of epithelial renewal. We next determined whether IL-6 was affecting epithelial renewal / proliferation and stem cell number *in vitro* through this pathway by utilising the Wnt inhibitor IWP2. We show that IWP2 abrogates the IL6-induced increase in both proliferation and the average number of buds per organoid compared to control (Figure 5A and B). The percentage of caspase 3 positive cells and organoid survival in the presence of IWP2 and / or IL-6 was comparable to control (Supplemental Figure 4).

Discussion

This work highlights a previously unrecognized role for autocrine IL-6 signaling during homeostasis in the small intestine. IL-6 stimulation was shown to increase *in vitro* crypt cell proliferation and stem cell number through the STAT3 signaling pathway. IL-6 activated pSTAT3 specifically in the nucleus of the Paneth cell through differential expression of the IL-6 receptor located on the Paneth cell basal membrane. IL-6 was also expressed in the crypt epithelium. Neutralizing IL-6 or blocking the IL-6 receptor with antibodies lowered basal organoid proliferation and crypt budding *in vitro* and reduced crypt stem and Paneth cell number *in vivo*. Use of the Wnt inhibitor IWP2 abrogated the IL-6 induced increase in organoid proliferation and crypt budding. These data suggest a role of autocrine IL-6 signaling and the Wnt signaling pathway in the regulation of crypt homeostasis.

Previous work using IL-6 receptor or IL-6 knockout mice demonstrated a role for IL-6 signaling in mouse models of inflammation and crypt epithelial cell survival and regeneration rather than homeostasis (11, 12, 14, 16, 24, 25). In agreement with other studies, we also showed that gut tissue from healthy IL-6 knockout mouse was similar to tissue from wild type mice (Supplemental Figure 2A-C). However, using a blocking antibody approach we demonstrated a previously unrecognised role for autocrine IL-6 signaling in the maintenance of crypt stem cell number (and Paneth cell number-see below) *in vivo*. These differences may be explained by redundancy effects known to occur in knockout mouse models and highlights the importance of interrogating this pathway using a variety of methods as has been shown in other studies (26).

Other groups have also implicated a role for IL-6 in maintaining homeostasis (27–29) as well as ageing (30–32). Our findings suggest that *classic signaling* is involved in crypt homeostasis; we show that addition of IL-6 to the basal side of crypts *in vitro* causes pSTAT3 activation in Paneth cells only and this correlates with the expression of the IL-6 receptor on the Paneth cell basal membrane. It has been suggested that anti-inflammatory / regenerative properties of IL-6 most likely depend on IL-6 *classic*- rather than *trans*-signaling (20, 33). Our studies concur with this; if binding of soluble IL-6 receptor to the ubiquitously expressed gp130 was occurring in our system then this would permit all cells of the crypt epithelium to express nuclear pSTAT3 in response to IL-6, an effect that we did not observe. The relative contribution of *classic* IL-6 signaling versus *trans* signaling in crypt homeostasis *versus* inflammation remains the focus of future work.

Our findings demonstrated that IL-6 mediated its *in vitro* effects on crypt cell proliferation and stem cells through the pSTAT3 pathway. Crypt cell proliferation in response to IL-6 exhibited a bell-shaped concentration response curve, which has previously been described (34). Epithelial STAT3 signaling pathway has shown to be key for small intestinal stem cell survival (35) and regeneration during intestinal mucosal wound healing (9, 13). Using full growth factor media and chronic STAT3 inhibition we also showed that epithelial STAT3 was important for *in vitro* crypt regeneration even in the absence of exogenous IL-6 (Supplemental Figure 1A). Interestingly we showed *in vivo* that low levels of nuclear pSTAT3 activation (Supplemental Figure 2J) were present in most UEA-1 positive Paneth cells at the base of small intestinal crypts; there was also evidence of a small number of crypts expressing high pSTAT3 activation in Paneth cells (Supplemental Figure 2K). These findings support the hypothesis that pSTAT3 signaling is dynamic and transient during homeostasis. In the future the development of fluorescent reporter systems would be required to study dynamic pSTAT3 signaling in real time.

The STAT3 signaling pathway can be activated by a number of cytokines including IL-6 and IL-22 (36, 37). Interestingly, activation of IL-22 rather than IL-6 was shown to be key in regulating epithelial STAT3 wound healing following dextran sodium sulfate-induced experimental colitis in mice (13) and in ameliorating gut inflammation (38). This highlights the complexity of STAT3 signaling and it is likely that fine tuning of this pathway through different cytokines exerts different functional responses depending on the context. Indeed, we showed that IL-22 stimulation of organoids resulted in global epithelial pSTAT3 activation (Supplemental Figure 3A), which was in contrast to the restricted activation in Paneth cells following IL-6 exposure. We also concur with previous findings (39) that IL-22 induces proliferation of both large and small intestinal organoids and affects organoid budding (Supplemental Figure 3); we also show that IL-6 can cause proliferation of colonic organoids. Whether the same mechanisms exist in the human gut epithelium remains to be elucidated. The relative contribution of different cytokines in regulating the STAT3 pathway in gut homeostasis *versus* inflammation and in the small intestine *versus* the colon is the subject of future investigation.

Although Paneth cells are not an absolute requirement for survival, proliferation and stem cell activity (40, 41), previous work has shown that they provide important regenerative signals for modulation of the crypt stem cell niche (2, 42). Future work will elucidate the identity of the Wnt pathway / s involved in IL-6 and STAT3 signaling in small intestinal crypt homeostasis. This study has also identified a novel role for the IL-6 signaling-axis in regulating Paneth cell number *in vivo*. Paneth cell metaplasia in the colon is a feature of IBD (43, 44), in addition to elevated levels of IL-6 in the serum and tissues (45, 46). We speculate that alterations in the IL-6 signaling axis may be a contributing factor to this phenotype. Furthermore, in the clinic, some rheumatoid arthritis patients treated with the IL-6 antibody tocilizumab display adverse side effects (47, 48) the mechanism by which this occurs is unknown.

IL-6 can also activate other signaling pathways not studied in this paper (17). This highlights the importance of understanding the complex biology of IL-6 during health and disease. Here we show a previously unrecognised role for IL-6 signaling in health. Understanding the

Europe PMC Funders Author Manuscripts

mechanisms of IL-6 regulation of crypt cell renewal has wider implications for the prevention or development of future treatments for inflammatory bowel disease. More targeted treatments for inflammatory disorders that retain *classic* IL-6 signaling and homeostatic levels of epithelial crypt renewal but inhibit *trans* IL-6 signaling (49) through specific cell types appears to be the ideal scenario for the future (50, 51).

Supplementary Material

Refer to Web version on PubMed Central for supplementary material.

Acknowledgements

The authors thank Prof. Alastair Watson, Mr. Simon Deakin and staff from the Disease Modelling Unit; and Dr. Paul Thomas from the Henry Wellcome Laboratory for Cell Imaging at the University of East Anglia.

¶The authors gratefully acknowledge the funding from the University of East Anglia, Biotechnology and Biological Sciences Research Council; Institute Strategic Programme for Integrated Biology of the Gastrointestinal Tract IFR/08/1 and Gut Health and Food Safety BB/J004529/1 (AS); the Boston Cancer and Leukaemia Fund (AS) and the Ministry of Health, Italy, GR-2011-02347991 (MC).

References

1. Barker N, van Es JH, Kuipers J, Kujala P, van den Born M, Cozijnsen M, Haegebarth A, Korving J, Begthel H, Peters PJ, Clevers H. Identification of stem cells in small intestine and colon by marker gene Lgr5. Nature. 2007; 449:1003–1007. [PubMed: 17934449]
2. Sato T, van Es JH, Snippert HJ, Stange DE, Vries RG, van den Born M, Barker N, Shroyer NF, van de Wetering M, Clevers H. Paneth cells constitute the niche for Lgr5 stem cells in intestinal crypts. Nature. 2011; 469:415–418. [PubMed: 21113151]
3. Reynolds A, Wharton N, Parris A, Mitchell E, Sobolewski A, Kam C, Bigwood L, El Hadi A, Munsterberg A, Lewis M, Speakman C, et al. Canonical Wnt signals combined with suppressed TGFbeta/BMP pathways promote renewal of the native human colonic epithelium. Gut. 2014; 63:610–621. [PubMed: 23831735]
4. Skoczek DA, Walczysko P, Horn N, Parris A, Clare S, Williams MR, Sobolewski A. Luminal microbes promote monocyte-stem cell interactions across a healthy colonic epithelium. J Immunol. 2014; 193:439–451. [PubMed: 24907348]
5. Brown SL, Riehl TE, Walker MR, Geske MJ, Doherty JM, Stenson WF, Stappenbeck TS. Myd88-dependent positioning of Ptgs2-expressing stromal cells maintains colonic epithelial proliferation during injury. J Clin Invest. 2007; 117:258–269. [PubMed: 17200722]
6. Pull SL, Doherty JM, Mills JC, Gordon JI, Stappenbeck TS. Activated macrophages are an adaptive element of the colonic epithelial progenitor niche necessary for regenerative responses to injury. Proc Natl Acad Sci U S A. 2005; 102:99–104. [PubMed: 15615857]
7. Seno H, Miyoshi H, Brown SL, Geske MJ, Colonna M, Stappenbeck TS. Efficient colonic mucosal wound repair requires Trem2 signaling. Proc Natl Acad Sci U S A. 2009; 106:256–261. [PubMed: 19109436]
8. Ayyaz A, Li H, Jasper H. Haemocytes control stem cell activity in the Drosophila intestine. Nat Cell Biol. 2015; 17:736–748. [PubMed: 26005834]
9. Jiang H, Patel PH, Kohlmaier A, Grenley MO, McEwen DG, Edgar BA. Cytokine/Jak/Stat signaling mediates regeneration and homeostasis in the Drosophila midgut. Cell. 2009; 137:1343–1355. [PubMed: 19563763]
10. Osman D, Buchon N, Chakrabarti S, Huang YT, Su WC, Poidevin M, Tsai YC, Lemaitre B. Autocrine and paracrine unpaired signaling regulate intestinal stem cell maintenance and division. Journal of cell science. 2012; 125:5944–5949. [PubMed: 23038775]
11. Grivennikov S, Karin E, Terzic J, Mucida D, Yu GY, Vallabhapurapu S, Scheller J, Rose-John S, Cheroutre H, Eckmann L, Karin M. IL-6 and Stat3 are required for survival of intestinal epithelial

Europe PMC Funders Author Manuscripts

cells and development of colitis-associated cancer. Cancer cell. 2009; 15:103–113. [PubMed: 19185845]

12. Jin X, Zimmers TA, Zhang Z, Pierce RH, Koniaris LG. Interleukin-6 is an important in vivo inhibitor of intestinal epithelial cell death in mice. Gut. 2010; 59:186–196. [PubMed: 19074180]
13. Pickert G, Neufert C, Leppkes M, Zheng Y, Wittkopf N, Warntjen M, Lehr HA, Hirth S, Weigmann B, Wirtz S, Ouyang W, et al. STAT3 links IL-22 signaling in intestinal epithelial cells to mucosal wound healing. J Exp Med. 2009; 206:1465–1472. [PubMed: 19564350]
14. Kuhn KA, Manieri NA, Liu TC, Stappenbeck TS. IL-6 stimulates intestinal epithelial proliferation and repair after injury. PLoS One. 2014; 9:e114195. [PubMed: 25478789]
15. Bollrath J, Phesse TJ, von Burstin VA, Putoczki T, Bennecke M, Bateman T, Nebelsiek T, Lundgren-May T, Canli O, Schwitalla S, Matthews V, et al. gp130-mediated Stat3 activation in enterocytes regulates cell survival and cell-cycle progression during colitis-associated tumorigenesis. Cancer cell. 2009; 15:91–102. [PubMed: 19185844]
16. Lee MJ, Lee JK, Choi JW, Lee CS, Sim JH, Cho CH, Lee KH, Cho IH, Chung MH, Kim HR, Ye SK. Interleukin-6 induces S100A9 expression in colonic epithelial cells through STAT3 activation in experimental ulcerative colitis. PLoS One. 2012; 7:e38801. [PubMed: 22962574]
17. Mihara M, Hashizume M, Yoshida H, Suzuki M, Shiina M. IL-6/IL-6 receptor system and its role in physiological and pathological conditions. Clinical science. 2012; 122:143–159. [PubMed: 22029668]
18. Hunter CA, Jones SA. IL-6 as a keystone cytokine in health and disease. Nat Immunol. 2015; 16:448–457. [PubMed: 25898198]
19. Garbers C, Aparicio-Siegmund S, Rose-John S. The IL-6/gp130/STAT3 signaling axis: recent advances towards specific inhibition. Current opinion in immunology. 2015; 34:75–82. [PubMed: 25749511]
20. Scheller J, Chalaris A, Schmidt-Arras D, Rose-John S. The pro- and anti-inflammatory properties of the cytokine interleukin-6. Biochimica et biophysica acta. 2011; 1813:878–888. [PubMed: 21296109]
21. Jones SA, Richards PJ, Scheller J, Rose-John S. IL-6 transsignaling: the in vivo consequences. Journal of interferon & cytokine research : the official journal of the International Society for Interferon and Cytokine Research. 2005; 25:241–253.
22. Sato T, Vries RG, Snippert HJ, van de Wetering M, Barker N, Stange DE, van Es JH, Abo A, Kujala P, Peters PJ, Clevers H. Single Lgr5 stem cells build crypt-villus structures in vitro without a mesenchymal niche. Nature. 2009; 459:262–265. [PubMed: 19329995]
23. Farin HF, Karthaus WR, Kujala P, Rakhshandehroo M, Schwank G, Vries RG, Kalkhoven E, Nieuwenhuis EE, Clevers H. Paneth cell extrusion and release of antimicrobial products is directly controlled by immune cell-derived IFN-gamma. J Exp Med. 2014; 211:1393–1405. [PubMed: 24980747]
24. Francois M, Birman E, Forner KA, Gaboury L, Galipeau J. Adoptive transfer of mesenchymal stromal cells accelerates intestinal epithelium recovery of irradiated mice in an interleukin-6-dependent manner. Cytotherapy. 2012; 14:1164–1170. [PubMed: 22574720]
25. Bernardo D, Vallejo-Diez S, Mann ER, Al-Hassi HO, Martinez-Abad B, Montalvillo E, Tee CT, Murugananthan AU, Nunez H, Peake ST, Hart AL, et al. IL-6 promotes immune responses in human ulcerative colitis and induces a skin-homing phenotype in the dendritic cells and Tcells they stimulate. Eur J Immunol. 2012; 42:1337–1353. [PubMed: 22539302]
26. Sommer J, Engelowski E, Baran P, Garbers C, Floss DM, Scheller J. Interleukin-6, but not the interleukin-6 receptor plays a role in recovery from dextran sodium sulfate-induced colitis. International journal of molecular medicine. 2014; 34:651–660. [PubMed: 24993179]
27. Giraud AS, Jackson C, Menheniott TR, Judd LM. Differentiation of the Gastric Mucosa IV. Role of trefoil peptides and IL-6 cytokine family signaling in gastric homeostasis. American journal of physiology. Gastrointestinal and liver physiology. 2007; 292:G1–5. [PubMed: 16935852]
28. Sims NA, Walsh NC. GP130 cytokines and bone remodelling in health and disease. BMB reports. 2010; 43:513–523. [PubMed: 20797312]

29. Jain U, Cao Q, Thomas NA, Woodruff TM, Schwaeble WJ, Stover CM, Stadnyk AW. Properdin provides protection from Citrobacter rodentium-induced intestinal inflammation in a C5a/IL-6-dependent manner. J Immunol. 2015; 194:3414–3421. [PubMed: 25725105]
30. Palin K, Moreau ML, Orcel H, Duvoid-Guillou A, Rabie A, Kelley KW, Moos F. Age-impaired fluid homeostasis depends on the balance of IL-6/IGF-I in the rat supraoptic nuclei. Neurobiology of aging. 2009; 30:1677–1692. [PubMed: 18255192]
31. Man AL, Gicheva N, Nicoletti C. The impact of ageing on the intestinal epithelial barrier and immune system. Cellular immunology. 2014; 289:112–118. [PubMed: 24759078]
32. Man AL, Bertelli E, Rentini S, Regoli M, Briars G, Marini M, Watson AJ, Nicoletti C. Age-associated modifications of intestinal permeability and innate immunity in human small intestine. Clinical science. 2015; 129:515–527. [PubMed: 25948052]
33. Becker C, Fantini MC, Schramm C, Lehr HA, Wirtz S, Nikolaev A, Burg J, Strand S, Kiesslich R, Huber S, Ito H, et al. TGF-beta suppresses tumor progression in colon cancer by inhibition of IL-6 trans-signaling. Immunity. 2004; 21:491–501. [PubMed: 15485627]
34. van Dam M, Mullberg J, Schooltink H, Stoyan T, Brakenhoff JP, Graeve L, Heinrich PC, Rose-John S. Structure-function analysis of interleukin-6 utilizing human/murine chimeric molecules. Involvement of two separate domains in receptor binding. The Journal of biological chemistry. 1993; 268:15285–15290. [PubMed: 8325898]
35. Matthews JR, Sansom OJ, Clarke AR. Absolute requirement for STAT3 function in small-intestine crypt stem cell survival. Cell death and differentiation. 2011; 18:1934–1943. [PubMed: 21637293]
36. Nguyen PM, Putoczki TL, Ernst M. STAT3-Activating Cytokines: A Therapeutic Opportunity for Inflammatory Bowel Disease? Journal of interferon & cytokine research : the official journal of the International Society for Interferon and Cytokine Research. 2015; 35:340–350.
37. Aden K, Breuer A, Rehman A, Geese H, Tran F, Sommer J, Waetzig GH, Reinheimer TM, Schreiber S, Rose-John S, Scheller J, et al. Classic IL-6R signalling is dispensable for intestinal epithelial proliferation and repair. Oncogenesis. 2016; 5:e270. [PubMed: 27869785]
38. Sugimoto K, Ogawa A, Mizoguchi E, Shimomura Y, Andoh A, Bhan AK, Blumberg RS, Xavier RJ, Mizoguchi A. IL-22 ameliorates intestinal inflammation in a mouse model of ulcerative colitis. J Clin Invest. 2008; 118:534–544. [PubMed: 18172556]
39. Lindemans CA, Calafiore M, Mertelsmann AM, O'Connor MH, Dudakov JA, Jenq RR, Velardi E, Young LF, Smith OM, Lawrence G, Ivanov JA, et al. Interleukin-22 promotes intestinal-stem-cell-mediated epithelial regeneration. Nature. 2015; 528:560–564. [PubMed: 26649819]
40. Kim TH, Escudero S, Shivdasani RA. Intact function of Lgr5 receptor-expressing intestinal stem cells in the absence of Paneth cells. Proc Natl Acad Sci U S A. 2012; 109:3932–3937. [PubMed: 22355124]
41. Durand A, Donahue B, Peignon G, Letourneur F, Cagnard N, Slomianny C, Perret C, Shroyer NF, Romagnolo B. Functional intestinal stem cells after Paneth cell ablation induced by the loss of transcription factor Math1 (Atoh1). Proc Natl Acad Sci U S A. 2012; 109:8965–8970. [PubMed: 22586121]
42. Farin HF, Jordens I, Mosa MH, Basak O, Korving J, Tauriello DV, de Punder K, Angers S, Peters PJ, Maurice MM, Clevers H. Visualization of a short-range Wnt gradient in the intestinal stem-cell niche. Nature. 2016; 530:340–343. [PubMed: 26863187]
43. Simmonds N, Furman M, Karanika E, Phillips A, Bates AW. Paneth cell metaplasia in newly diagnosed inflammatory bowel disease in children. BMC gastroenterology. 2014; 14:93. [PubMed: 24885054]
44. Tanaka M, Saito H, Kusumi T, Fukuda S, Shimoyama T, Sasaki Y, Suto K, Munakata A, Kudo H. Spatial distribution and histogenesis of colorectal Paneth cell metaplasia in idiopathic inflammatory bowel disease. Journal of gastroenterology and hepatology. 2001; 16:1353–1359. [PubMed: 11851832]
45. Mudter J, Neurath MF. Il-6 signaling in inflammatory bowel disease: pathophysiological role and clinical relevance. Inflammatory bowel diseases. 2007; 13:1016–1023. [PubMed: 17476678]
46. Waldner MJ, Neurath MF. Master regulator of intestinal disease: IL-6 in chronic inflammation and cancer development. Semin Immunol. 2014; 26:75–79. [PubMed: 24447345]

47. Gout T, Ostor AJ, Nisar MK. Lower gastrointestinal perforation in rheumatoid arthritis patients treated with conventional DMARDs or tocilizumab: a systematic literature review. Clinical rheumatology. 2011; 30:1471–1474. [PubMed: 21833686]

48. Emery P, Keystone E, Tony HP, Cantagrel A, van Vollenhoven R, Sanchez A, Alecock E, Lee J, Kremer J. IL-6 receptor inhibition with tocilizumab improves treatment outcomes in patients with rheumatoid arthritis refractory to anti-tumour necrosis factor biologicals: results from a 24-week multicentre randomised placebo-controlled trial. Annals of the rheumatic diseases. 2008; 67:1516–1523. [PubMed: 18625622]

49. Rose-John S. IL-6 trans-signaling via the soluble IL-6 receptor: importance for the pro-inflammatory activities of IL-6. International journal of biological sciences. 2012; 8:1237–1247. [PubMed: 23136552]

50. Matsumoto S, Hara T, Mitsuyama K, Yamamoto M, Tsuruta O, Sata M, Scheller J, Rose-John S, Kado S, Takada T. Essential roles of IL-6 trans-signaling in colonic epithelial cells, induced by the IL-6/soluble-IL-6 receptor derived from lamina propria macrophages, on the development of colitis-associated premalignant cancer in a murine model. J Immunol. 2010; 184:1543–1551. [PubMed: 20042582]

51. Schaper F, Rose-John S. Interleukin-6: Biology, signaling and strategies of blockade. Cytokine & growth factor reviews. 2015; 26:475–487. [PubMed: 26189695]

Europe PMC Funders Author Manuscripts

Europe PMC Funders Author Manuscripts

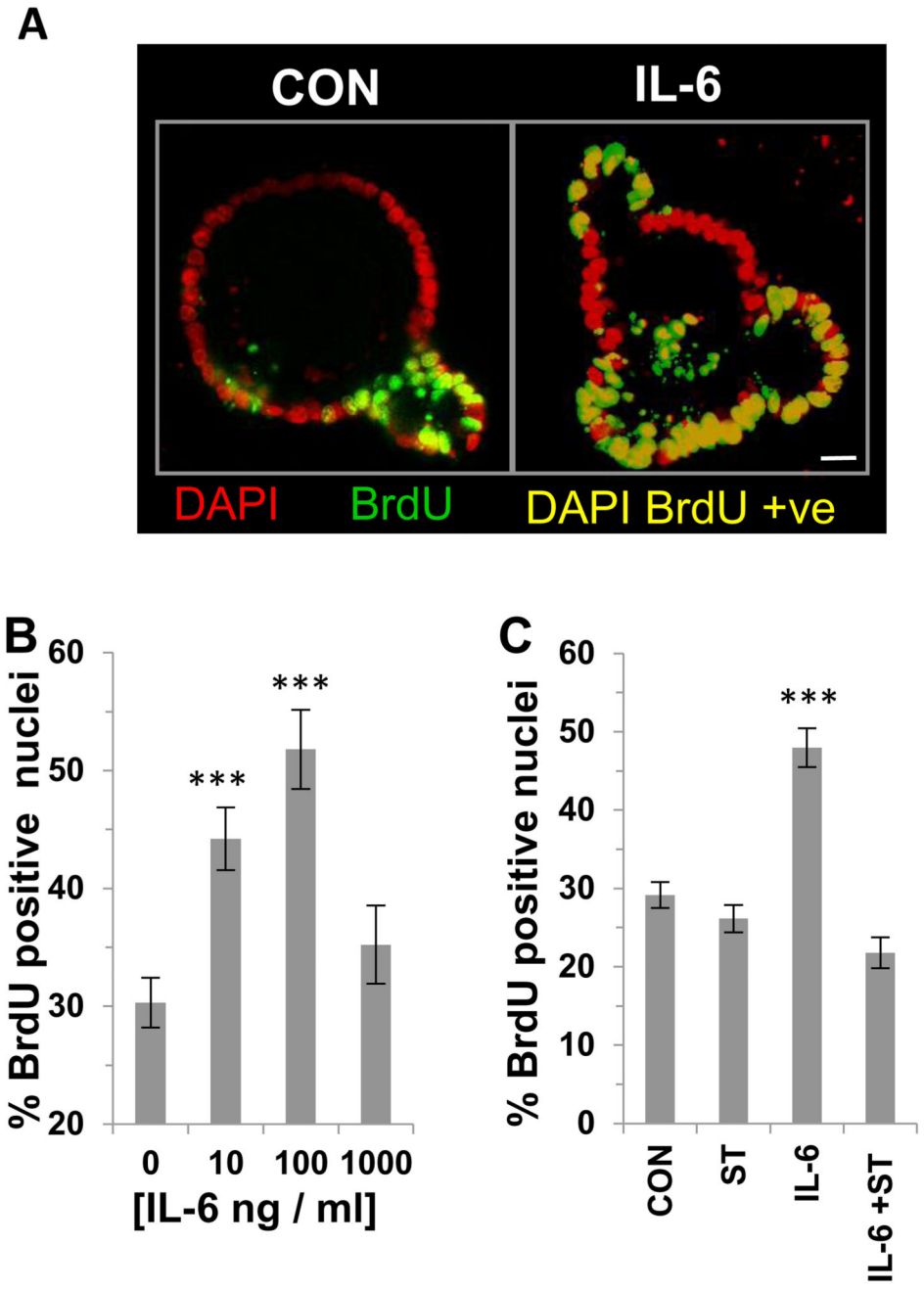

Figure 1. IL-6 stimulates proliferation of small intestinal organoids *via* a STAT3-mediated signaling pathway.

(**A**) Representative confocal images of BrdU incorporation (green) into the nuclei (DAPI; red) of small intestinal organoids cultured in the absence or presence of IL-6 (100 ng / ml). DAPI BrdU positive cells (yellow) Scale bar 10μm. (**B**) Histogram showing the percentage of BrdU positive nuclei in mouse small intestinal organoids following 24 hours IL-6 (10-1000 ng / ml) stimulation compared to control (n=3, ***P<0.001). (**C**) Histogram showing percentage of BrdU positive nuclei in mouse small intestinal organoids following

24 hour IL-6 stimulation (100 ng / ml) in the presence or absence of STATTIC and compared to control (n=3, ***P<0.001).

Europe PMC Funders Author Manuscripts

Europe PMC Funders Author Manuscripts

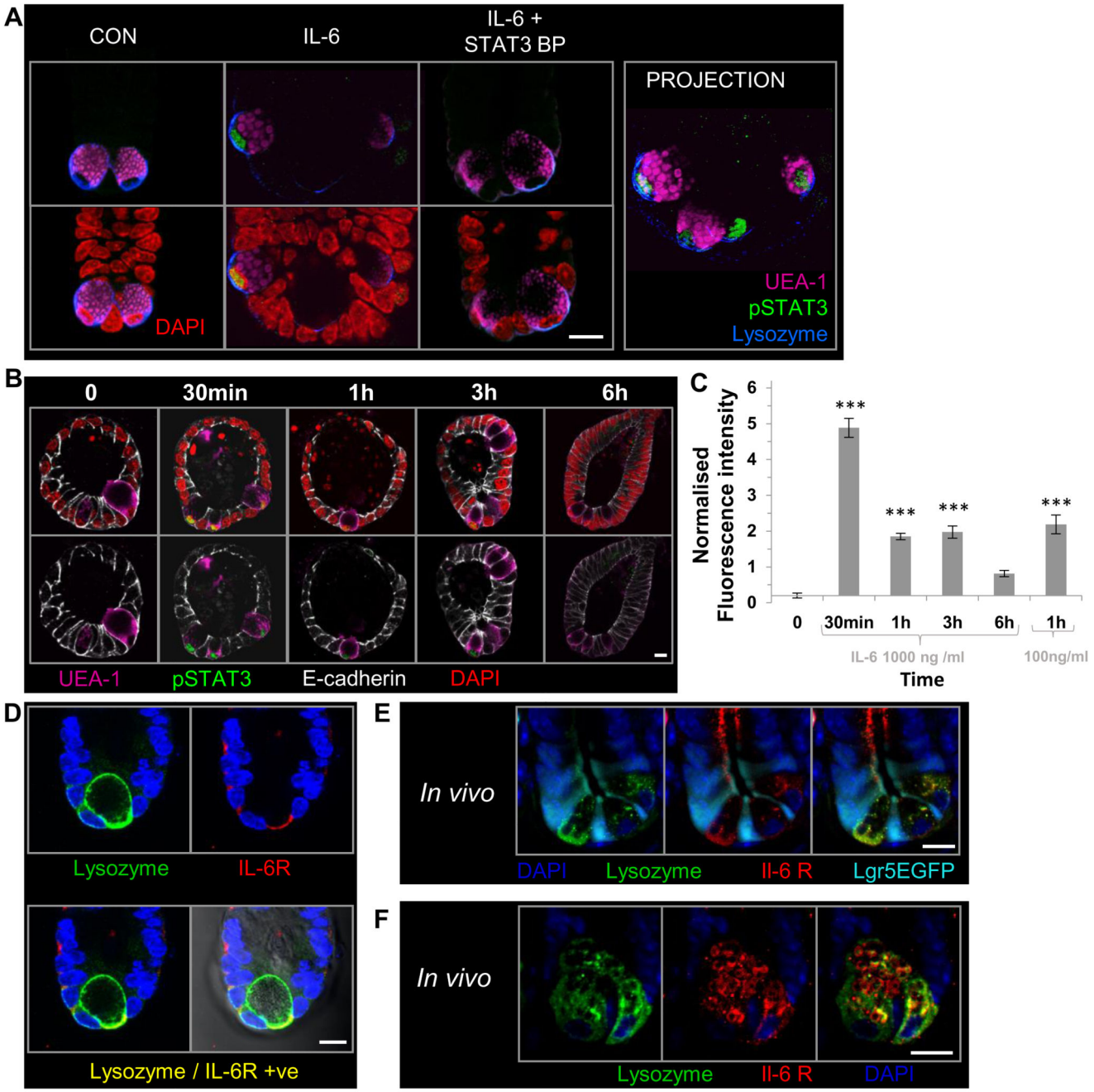

Figure 2. IL-6 induces activation of nuclear pSTAT3 in Paneth cells of the small intestine through differential expression of the IL-6 receptor.

(**A**) Representative confocal images showing the presence of pSTAT3 immunofluorescent labelling (green) in the nuclei (DAPI; red) of UEA-1 (pink), lysozyme (blue) positive Paneth cells in organoids following 1 hour IL-6 (100 ng / ml) stimulation in the presence or absence of a pSTAT3 blocking peptide. (**B**) Representative confocal images of pSTAT3 (green) in the nuclei (DAPI; red) of UEA-1 (pink) positive cells in organoids stimulated with IL-6 (1000 ng / ml) for 0-6 hours. E-cadherin-white. (**C**) Histogram showing the time course of IL-6

induced pSTAT3 activation in UEA-1 positive cells from 0 to 6 hours post-stimulation using 1000 or 100 ng /ml. Data expressed as fluorescence intensity (a.u) and normalised to control UEA-1 positive nuclei. (n=3, ***P<0.001). (**D**) Representative confocal images showing immunofluorescent labelling of IL-6 receptor localisation (red) in lysozyme (green) positive cells in small intestinal organoid culture. (**E**) and (**F**) Representative confocal images of small intestine taken from Lgr5EGFP mice showing IL-6 receptor localisation (red) on the basal membrane of lysozyme positive cells (**E**) and intracellular granules (**F**); Lgr5EGFP (cyan) and lysozyme positive cells (green). Confocal imaging data is representative of n=3 independent experiments. Scale bar 10 μm.

Europe PMC Funders Author Manuscripts

Europe PMC Funders Author Manuscripts

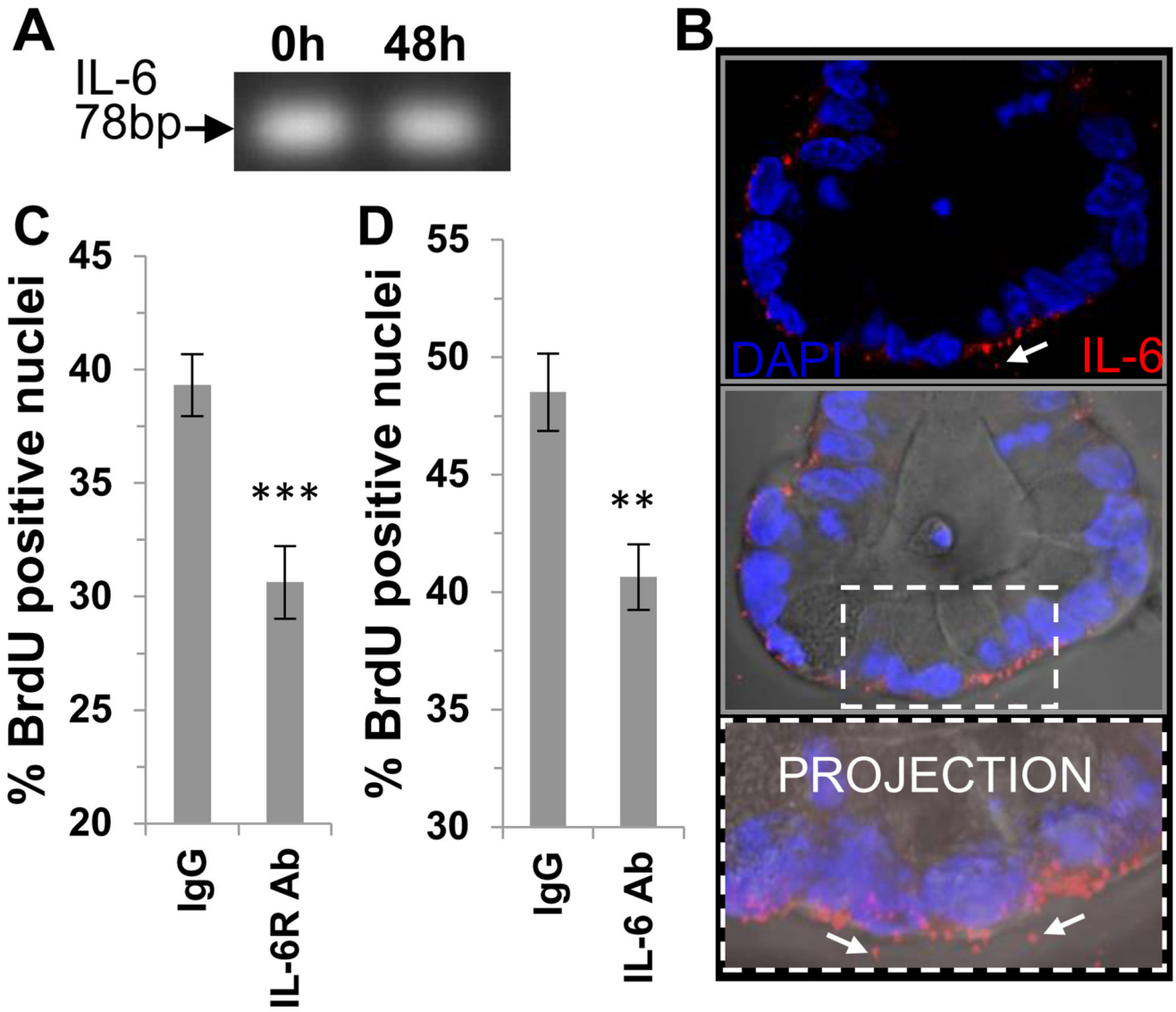

Figure 3. Autocrine IL-6 signaling regulates small intestinal organoid proliferation.

(**A**) PCR gel showing IL-6 transcript expression in *in vivo* / freshly isolated (0 h) and cultured (48 h) small intestinal crypts (**B**) Representative confocal image showing immunofluorescent labelling of IL-6 (red), nuclei (DAPI blue) of small intestinal organoids with the DIC image overlayed and associated projection image *in vitro*. White arrows indicate extracellular pools of IL-6. Scale bar 10 μm. (**C**) Histogram showing percentage positive BrdU positive nuclei in mouse small intestinal organoids in the presence of an IL-6 receptor blocking antibody (n=3, **P<0.01) and (**D**) an IL-6 neutralising antibody (n=3, ***P<0.001) compared to respective IgG control. Data are represented as mean +/- SEM.

Europe PMC Funders Author Manuscripts

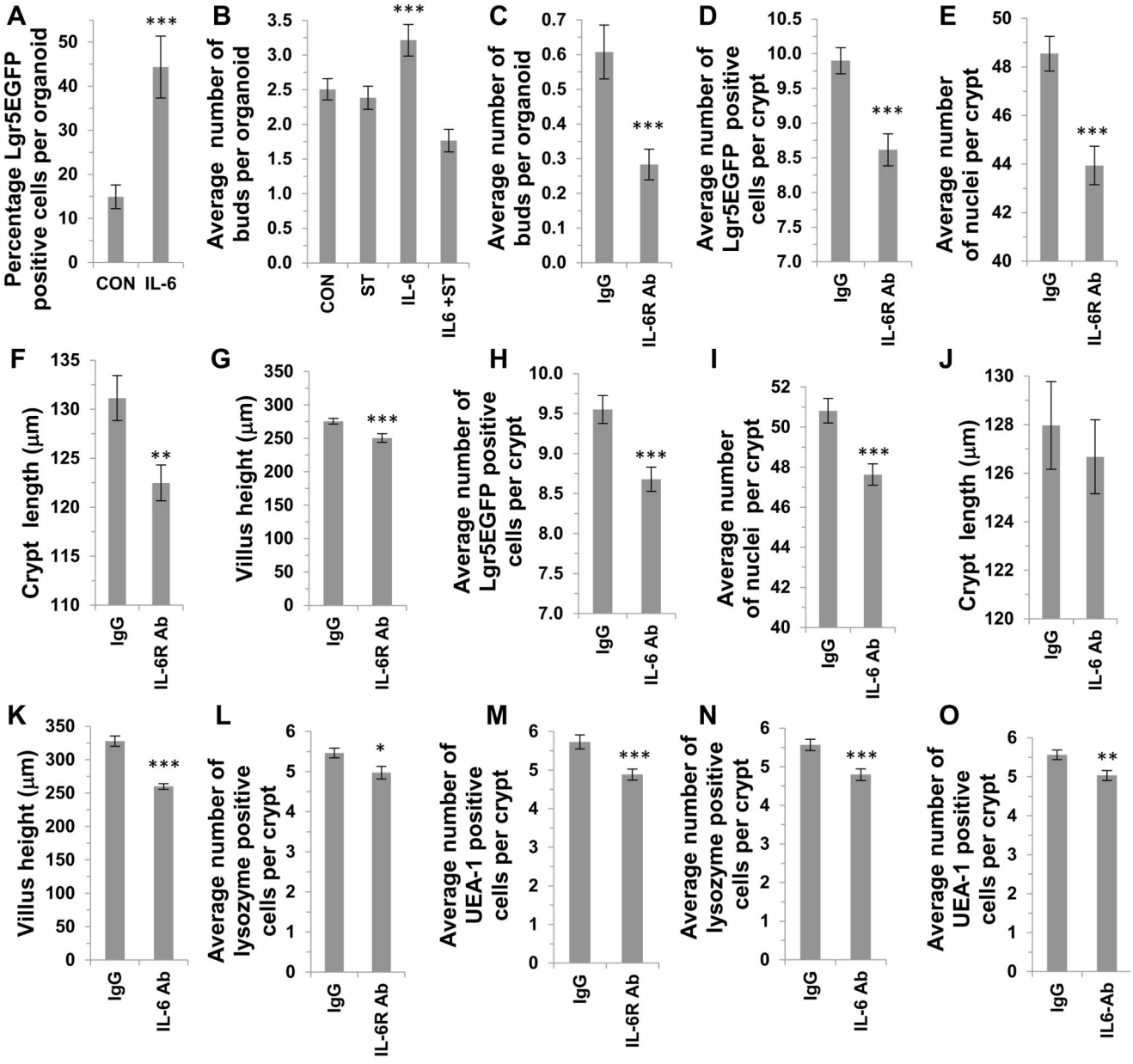

Figure 4. IL-6 receptor signaling modulates Lgr5EGFP^{+} crypt stem cell number *in vitro* and *in vivo*.

(**A**) Histogram showing the effect of IL-6 (100 ng / ml) treatment on the percentage of Lgr5EGFP positive cells per crypt organoid compared to control (n=3, ***P<0.001). (**B**) Histogram showing the average number of buds per crypt organoid following IL-6 (100 ng / ml) treatment (n=3, ***P<0.001), or treatment with STATTIC (20 μM). (**C**) Histogram showing the average number of buds per organoid *in vitro* when cultured in the presence of an IL-6 receptor blocking antibody (n=3, ***P<0.001) compared to IgG control. (**D**) Histogram showing the average number of Lgr5EGFP positive stem cells per crypt (**E**) the average number of nuclei per crypt, (**F**) the crypt length and (**G**) the villus height in the small intestine of mice treated with a IL-6 receptor blocking antibody compared to

respective IgG controls (n=3, ***P<0.001; **P<0.01). (**H**) Histogram showing the average number of Lgr5EGFP positive stem cells per crypt, (**I**) the average number of nuclei per crypt, (**J**) the average crypt length and (**K)** the average villus height in the small intestine of mice treated with a IL-6 neutralising antibody (n=3, ***P<0.001). Histograms showing the *in vivo* effect of an IL-6 receptor blocking antibody on the number of (**L**) lysozyme or (**M**) UEA-1 positive cells per crypt compared to IgG controls (n=3, *P<0.05; ***P<0.001 respectively). Histograms showing the effect of an IL-6 neutralising antibody on the number of (**N**) lysozyme or (**O**) UEA-1 positive cells per small intestinal crypt compared to IgG controls (n=3, ***P<0.001; **P<0.01 respectively). Data are represented as mean +/- SEM.

Europe PMC Funders Author Manuscripts

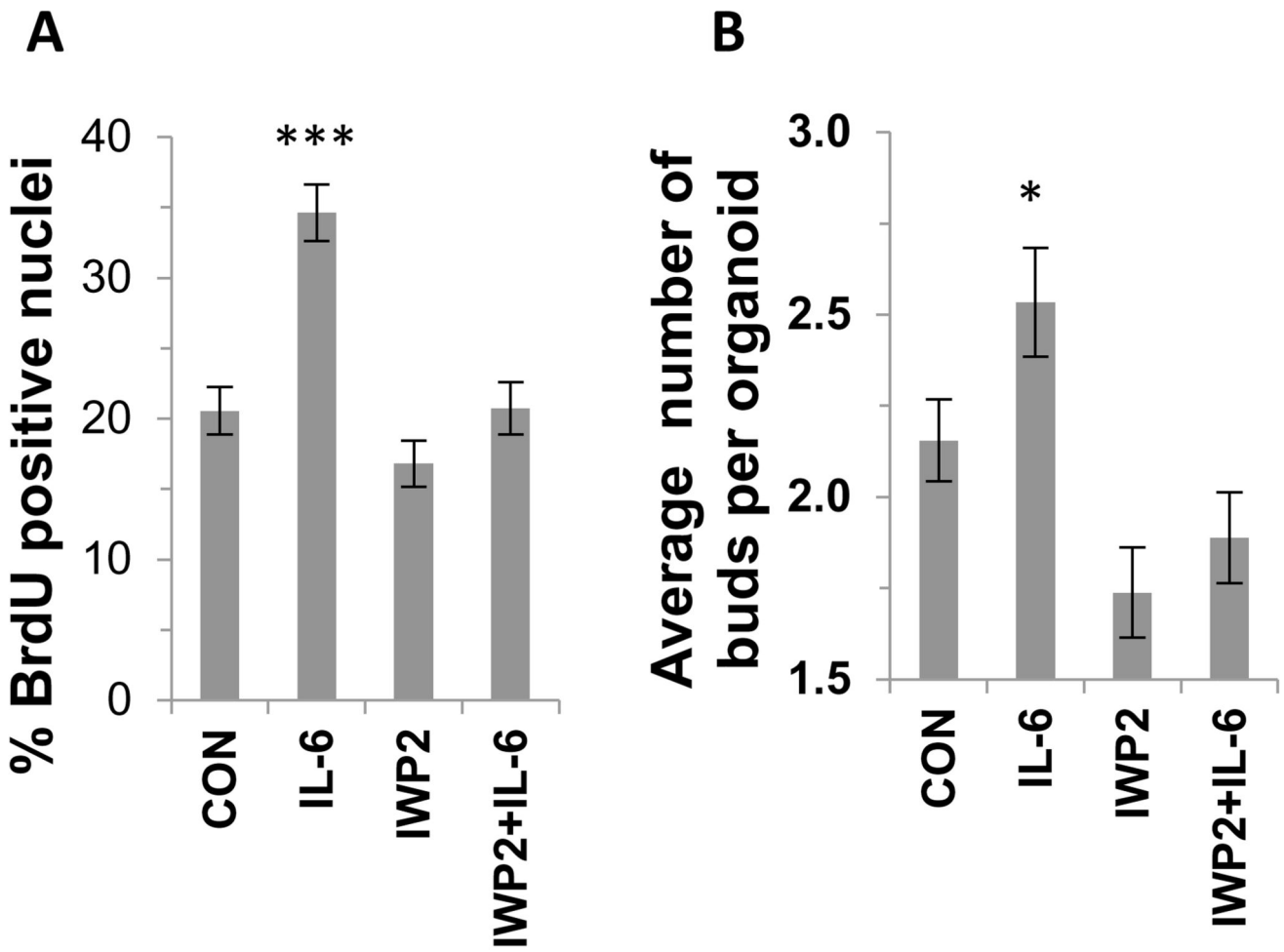

Figure 5. Wnt inhibition abrogates the IL-6-induced proliferation and budding of small intestinal organoids.

Histograms showing the effect of IWP2 on (**A**) the percentage of BrdU positive crypt nuclei (n=3, ***P<0.001) and (**B**) the average number of buds per crypt organoid following IL-6 stimulation (n=3, *P<0.05). Data are represented as mean +/- SEM.